Analysis of laminated glass beams using the Strong Discontinuities Approach

Loredana Contrafatto[1], Giuseppe Tommaso Di Venti[1]
[1] *Department of Civil and Environmental Engineering, University of Catania, Italy*
E-mail: loredana.contrafatto@dica.unict.it, diventi@dica.unict.it

Keywords: Interfaces, Strong Discontinuities, Laminated Glass Unit.

SUMMARY.Failure of laminated glass units is characterized by the growth and propagation of interfaces that can arise in unpredictable location of the layers. The paper presents the application of a theoretical model suitable in predicting the fracture path across the layers of laminated glass units when subjected to a static transversal load. The model falls in the context of the Strong Discontinuities Approach (SDA). The numerical implementation in the Finite Element Method is based on Elements with Embedded Discontinuities concept. All the relevant equations of the model are obtained from a variational principle formulated in a general context, thus allowing also for nonlinear continua. Relevant applications to laminated glass beams are presented.

1 INTRODUCTION

Glass is being increasingly used as a structural material. In particular, its favorable aesthetic qualities have made it popular with modern designers. The most recent developments have seen glass being used as major structural elements such as beams and columns. Laminated glass elements for structural applications consist of two or more ply of glass bonded together by a thin interlayer, usually PolyVinyl Butyral (PVB). The assembly presents some advantages over monolithic glass of the same nominal thickness with respect to impact resistance and post fracture behavior. The failure is dominated by a lot of factors such as thickness of the ply and of the interlayer, temperature, composition of the interlayer. Despite the increased use of laminated glass, research has focused mainly on monolithic glass, while fewer efforts were devoted to laminated glass. More specifically, to date, experimental data on laminated glass exist, while theoretical models are scarce. Moreover, existing theoretical analyses are restricted by additional simplifying assumptions based on the intuitive evaluation that the actual structural behavior of the laminated glass beam lies somewhere between two limiting cases: the layered limit and the monolithic limit.

Analytical models that predict stress development and ultimate strength of laminated glass beams and plates have been presented in [1, 2, 3, 4]. However the analysis of breakage and the prediction of crack paths are not frequent in the literature. For instance, in [5] an analytical model based on cumulative damage theory is discussed for the prediction of the cumulative probabilities of inner glass ply breakage. Taking into account that on the whole glass units exhibit a damaging-fracturing behavior and discontinuities in the displacement field can arise in unpredictable locations, it seems possible that the problem can be studied in a different area. Indeed, this phenomena can be effectively described by means of mechanical models that incorporate the kinematics of strong discontinuities obtained by an enrichment of the displacement field with a discontinuous term. Consequently, the strain field is decomposed into a compatible and an enhanced term.

This paper shows the application of a model [6] in the context on the Strong Discontinuities Approach (SDA) [7, 8] to simply supported laminated glass beams. The numerical procedure used allows one to predict the fracture path inside and across the layers. The Finite Element implementation of the algorithm is based on the Elements with Embedded Discontinuities [9]. It follows recently

developed strategies exploiting the formal analogy between the equations of the enriched continuum and the theory of classical plasticity [10]. The growth and the propagation of interfaces is ruled by specific activation functions for each material of the units, based on cohesive fracture like criteria. In this way it obtains a structure of the numerical algorithm that allows the use of the procedure inside classical F.E. codes for the equilibrium problem of elastic-plastic solids. The model does not account for temperature gradients. In the applications both the flexural behavior of the beams and the growth and propagation of interfaces inside the glass layers and across the polymeric interlayer are investigated.

2 KINEMATICS OF STRONG DISCONTINUITIES

In this section the equations characterizing the kinematics associated with the Strong Discontinuity Approach (SDA) are summarized.

Let S be an interface embedded within a continuous body occupying the domain $\Omega \subset \Re^3$. We will limit the present discussion to the case of a single interface. The unit normal vector $\mathbf{n}$ is defined on the surface S. Let's introduce a domain $\Omega_\varphi \subset \Omega$ such that: $S \in \Omega_\varphi$ and S divides Ω_φ in two subdomains, $\Omega_\varphi^+, \Omega_\varphi^-$ (Figure 1). The normal $\mathbf{n}$ is oriented toward the interior of Ω_φ^+. The boundary of Ω_φ is divided by the surface S in two parts, $\partial\Omega_\varphi^+$, $\partial\Omega_\varphi^-$. According to the position of the interface, part of the boundary of Ω_φ can belong to $\partial\Omega = \partial\Omega_u \bigcup \partial\Omega_q$ (Figure 1(b)).

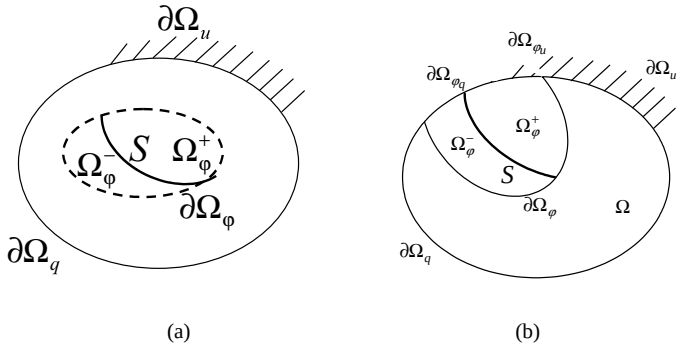

Figure 1: Domain Ω and enhanced region Ω_φ.

Across the interface S the displacement field can be discontinuous and the jump will be denoted by $[\![\mathbf{u}]\!]_S$. The displacement field in the continuum is described according to the format

$$\mathbf{u}(\mathbf{x},t) = \hat{\mathbf{u}}(\mathbf{x},t) + \tilde{\mathbf{u}}(\mathbf{x},t) \tag{1}$$

where $\bar{\mathbf{u}}$ is a continuous differentiable function defined in Ω, and $\tilde{\mathbf{u}}$ is a function having as support Ω_φ, continuous and differentiable everywhere except on the interface S and such that

$$\tilde{\mathbf{u}}^+(\mathbf{x},t) - \tilde{\mathbf{u}}^-(\mathbf{x},t) = [\![\mathbf{u}]\!]_S(\mathbf{x},t) \quad \forall \mathbf{x} \in S \tag{2}$$

$$\tilde{\mathbf{u}}(\mathbf{x},t) = 0 \quad \text{on} \quad \partial\Omega_\varphi \tag{3}$$

In this way the displacement field $\mathbf{u}$ is continuous everywhere except on the surface S. The function $\tilde{\mathbf{u}}$ can be given in the general form

$$\tilde{\mathbf{u}}(\mathbf{x},t) = \bar{M}_S(\mathbf{x})[\![\mathbf{u}]\!](\mathbf{x},t) \tag{4}$$

The enhanced enrichment function $\bar{M}_S(\mathbf{x})$ vanishes on the boundary of Ω_φ and on the restrained boundary $\partial\Omega_u$ and presents an unit jump across S. Function $[\![\mathbf{u}]\!](\mathbf{x},t)$ is a regular function, such that $[\![\mathbf{u}]\!] = [\![\mathbf{u}]\!]_S$ on S.

The enhanced enrichment function $\bar{M}_S(\mathbf{x})$ is given by

$$\bar{M}_S(\mathbf{x}) = \bar{N}_S(\mathbf{x})(H_S - \varphi(\mathbf{x})) \tag{5}$$

H_S being the Heaviside function related to the surface S and defined on the domain Ω_φ. Function $\varphi(\mathbf{x})$ is continuous, differentiable, defined in Ω_φ and such that

$$\varphi(\mathbf{x}) = \begin{cases} 0 & \forall \mathbf{x} \in \partial\Omega_\varphi^- \\ 1 & \forall \mathbf{x} \in \partial\Omega_\varphi^+ \end{cases} \tag{6}$$

Function $\bar{N}_S(\mathbf{x})$ takes the role of annihilating the enhanced displacement field along the restrained portion of the boundary $\partial\Omega_\varphi$, so that $\bar{N}_S(\mathbf{x}) = 1, \forall \mathbf{x} \notin \partial\Omega_{\varphi_u}$.

In Finite Element approximation the domain Ω is discretized in m finite elements. The Strong Discontinuities Approach approach is based on two assumptions: the domain Ω_φ coincides with the band of elements that are cut by the discontinuity and the interpolation of function $[\![\mathbf{u}]\!]$ is made element-wise. In this way, the nodal degrees of freedom coincide with the nodal displacements, and the jump function can be treated as an internal variable.

In the case of a constant jump $[\![\mathbf{u}]\!](\mathbf{x})$, the discretized displacements are given by:

$$\mathbf{u}(\mathbf{x}) = \sum_{i \in N_m} N_i(\mathbf{x})\hat{\mathbf{u}}_i + [\![\mathbf{u}]\!] \left[H_S(\mathbf{x}) - \sum_{j \in {S_m}^+} N_j(\mathbf{x}) \right] \bar{N}_S(\mathbf{x}) \tag{7}$$

where N_i are the shape functions defining the approximation of the displacement field, $\hat{\mathbf{u}}_i$ are nodal degrees of freedom, and the first sum is extended over the set N_m of all the nodes of the finite element mesh, while ${S_m}^+$ is the set of the enriched nodes belonging to $\Omega_\varphi \cap \Omega_\varphi^+$.

It has to be noted that, for an arbitrary choice of the domain Ω_φ, the nodal degrees of freedom do not have the physical meaning of the FEM nodal displacements and this makes difficult the application of the displacement boundary conditions.

3 THE MODEL

The kinematics defined in section 2 is used to develop a structural model for the simulation of growth and propagation of interface inside a continuum medium. The basic equations are derived following a variational approach. Specific constitutive hypotheses for the glass and interlayer are assumed.

3.1 Weak formulation

A general formulation in which the medium and the interface are ruled by different constitutive equations, defined by distinct free energy and dissipation functionals is considered. The variational formulation of the problem is derived starting from a generalized mixed multi-fields Hu-Washizu functional Π^{HW}, considering an elastic-plastic damaging behavior for both the bulk and the interface:

$$\Pi^{HW}\left(\sigma,\chi,\zeta,\mathbf{r},\mathbf{t}_S,\chi_S,\zeta_S,\hat{\mathbf{u}},\tilde{\mathbf{u}},\varepsilon_e,\alpha_e,\omega_e,\dot{\varepsilon}_p,\dot{\alpha}_p,\dot{\omega}_p,[\![\dot{\mathbf{u}}]\!]_{S_p},\dot{\alpha}_{S_p},\dot{\omega}_{S_p}\right) \tag{8}$$

in which the enhanced displacement field $\tilde{\mathbf{u}}$ and the internal plastic variables α_p, α_{S_p} and their conjugated internal forces χ, χ_S in the continuum and on the interfaces are introduced. Damage is described by the kinematic and dual variables (ω,ζ), (ω_S,ζ_S) respectively. The general formulation is particularized to the case of elastic medium and dissipative interfaces. In that case the internal variable in the bulk (α,ω) and their conjugated variables (χ,ζ) disappear. Using the kinematics of section 2, functional Π^{HW} takes the expression:

$$\begin{aligned}\Pi^{HW} = &\int_{\Omega/S}\sigma\cdot(\nabla^S\hat{\mathbf{u}}+\nabla^S\tilde{\mathbf{u}}-\varepsilon_e)d\Omega-\int_S\chi_S\cdot\left(\alpha_{S_e}+\alpha_{S_{p_0}}+\dot{\alpha}_{S_p}\Delta t\right)dS\\
&+\int_S\mathbf{t}_S\cdot\left(\Delta\tilde{\mathbf{u}}-[\![\mathbf{u}]\!]_{S_e}-[\![\mathbf{u}]\!]_{S_{p_0}}-[\![\dot{\mathbf{u}}]\!]_{S_p}\Delta t\right)dS+\int_{\Omega/S}\phi(\varepsilon_e)d\Omega\\
&+\int_S\phi_S([\![\mathbf{u}]\!]_{S_e},\alpha_{S_e})dS+\int_S d_S([\![\dot{\mathbf{u}}]\!]_{S_p},\dot{\alpha}_{S_p})\Delta t dS\\
&-\int_{\Omega/S}\mathbf{b}\cdot\mathbf{u}d\Omega-\int_{\partial(\Omega/S)_q}\mathbf{q}\cdot\mathbf{u}ds-\int_{\partial(\Omega/S)_u}\mathbf{r}\cdot(\mathbf{u}-\bar{\mathbf{u}})\,ds\end{aligned} \tag{9}$$

where the additive decomposition for the internal variables $[\![\mathbf{u}]\!]_S$ and α_S has been assumed:

$$\begin{aligned}[\![\mathbf{u}]\!]_S &= [\![\mathbf{u}]\!]_{S_e}+[\![\mathbf{u}]\!]_{S_p}=[\![\mathbf{u}]\!]_{S_e}+[\![\mathbf{u}]\!]_{S_{p_0}}+[\![\dot{\mathbf{u}}]\!]_{S_p}\Delta t\\
\alpha_S &= \alpha_{S_e}+\alpha_{S_p}=\alpha_{S_e}+\alpha_{S_{p_0}}+\dot{\alpha}_{S_p}\Delta t\end{aligned} \tag{10}$$

By eliminating variables $\varepsilon_e,\alpha_{S_e},[\![\dot{\mathbf{u}}]\!]_{S_p},\dot{\alpha}_{S_p}$ and performing appropriate Legendre transformations, the generalized Hellinger-Reissner functional Π^{HR} is obtained [6], whose stationarity conditions gives the relevant equations of the model:

$$\begin{array}{lcll}
\delta_{\hat{\mathbf{u}}}\Pi^{HR} & \Rightarrow & \left\{\begin{array}{lll} div\sigma+\mathbf{b}=0 & in & \Omega/S\\ \sigma\mathbf{n}=\mathbf{q} & on & \partial\Omega_q\\ \sigma\mathbf{n}=\mathbf{r} & on & \partial\Omega_u\end{array}\right. & \\
\delta_{\tilde{\mathbf{u}}}\Pi^{HR} & \Rightarrow & \mathbf{t}_S=\sigma\mathbf{n} & on\quad S\\
\delta_\sigma\Pi^{HR} & \Rightarrow & \nabla^S\hat{\mathbf{u}}+\nabla^S\tilde{\mathbf{u}}=\nabla_\sigma\phi'(\sigma) & in\quad \Omega/S\\
\delta_{\mathbf{t}_S}\Pi^{HR} & \Rightarrow & \triangle\tilde{\mathbf{u}}+\nabla_{\mathbf{t}_S}\phi'_S(\mathbf{t}_S,\chi_S)+\nabla_{\mathbf{t}_S}d'_S(\mathbf{t}_S,\chi_S)-\alpha_{S_{p_0}} & on\quad S\\
\delta_{\chi_S}\Pi^{HR} & \Rightarrow & -\nabla_{\chi_S}\phi'_S(\mathbf{t}_S,\chi_S)-\nabla_{\chi_S}d'_S(\mathbf{t}_S,\chi_S)-\alpha_{S_{p_0}}=0 & on\quad S\\
\delta_{\mathbf{r}}\Pi^{HR} & \Rightarrow & \hat{\mathbf{u}}+\tilde{\mathbf{u}}=\bar{\mathbf{u}} & on\quad \partial\Omega_u
\end{array} \tag{11}$$

The weak formulation is obtained discretizing the displacement fields appearing in Π^{HR}, resolving the internal variables at constitutive level and assuming linear elastic constitutive equations for the continuum. It allows an effective numerical implementation of the interface model able to predict both the occurrence of the discontinuity and its direction [11, 12]; no tracking algorithm is introduced. Among the many possible algorithmic frameworks, the one recently proposed in [10], based on the formal analogy between the enriched continuum and the theory of classical plasticity, has been implemented in the FEAP code [13].

3.2 Constitutive hypothesis

In the paper an elastic continuum medium is considered, both for the glass and interlayer, in which interfaces have a dissipative behavior.

For each material the deformation energy is given by the sum of two contributions:

$$\Pi(\varepsilon_e, \alpha_{S_e}) = \phi(\varepsilon_e) + \phi_S(\alpha_{S_e}) \tag{12}$$

where the first term is the standard elastic energy while the second term is the hardening energy, different from zero only in the region Ω_φ, for which the following quadratic form is assumed:

$$\phi_S(\alpha_{S_e}) = \int_S \frac{1}{2} H \alpha_{S_e}^2 dS \tag{13}$$

H being the finite softening modulus of the interface and α_{S_e} the softening internal variable.

In this work the dissipation is null throughout the bulk while the interface dissipative behavior is ruled by simple cohesive fracture-like models. The jump $[\![\mathbf{u}]\!]$ has not reversible component, so that $[\![\mathbf{u}]\!] = [\![\mathbf{u}]\!]_{S_p}$. Specifically, the following activation condition is used:

$$f(\mathbf{t}_S, \chi_S) = \mathbf{t}_{S_n} + k[\mathbf{t}_{S_m}^2]^b - f_{tu} + \chi_S \tag{14}$$

$\mathbf{t}_S$,$\mathbf{t}_{S_n}$ and $\mathbf{t}_{S_m}$ being respectively the stress on the surface S and its normal and tangential component, k and b being two parameters ruling the sharpness of the limit curve, f_{tu} being the tensile strength of the material. In (14) χ_S is the internal scalar force defined only on the surface S that rules the evolution of the limit surface, conjugated to the internal kinematic variable α_{S_e}.

The constitutive law for the kinematic internal interface variable α_{S_e} is such that the cohesive fracture dissipation energy is equal to the fracture energy of the material. For instance a linear or an exponential law can be used:

$$\chi_S = -\frac{f_{tu}^2}{2G_f}\alpha_{S_e} \qquad \chi_S = f_{tu}(1 - e^{\frac{f_{tu}\alpha_{S_e}}{G_f}}) \tag{15}$$

G_f being the fracture energy.

4 APPLICATIONS TO LAMINATED GLASS UNITS

The model of section 3 has been applied to simulate the behavior of simply supported two-ply laminated glass beams. The interfaces growth is assimilated to flexural cracks opening in the glass and to shear slip in the interlayer.

The laminated composite beam is characterized by two layers of thin glasses and one layer of PVB, as it is shown in fig. 2.

A numerical three point bending test has been performed. According to geometrical and material data from [14], the span length L of the beam is 0.8 m; the cross section width is 10 cm, the glass thickness is 5 mm for both the layers and the interlayer thickness is 0.38 mm. Glass elastic modulus and interlayer shear modulus are taken as 64.5 GPa and 1287 kPa, respectively. The Poisson's ratio of glass and PVB are taken to be 0.23 and 0.49, respectively. An increasing prescribed displacement is applied at mid-span. The activation function (14) is specialized as in table 1.

In fig. 3 the prediction of the initial crack and its evolution in the layers is shown. Specifically the zoom in the midspan of the internal softening variable α_{S_p} is depicted. No interpolation inside the element is introduced in the graph so that the actual value at the Gauss points is represented. The interfaces begin at the midpoint of the bottom beam and propagate along the vertical direction

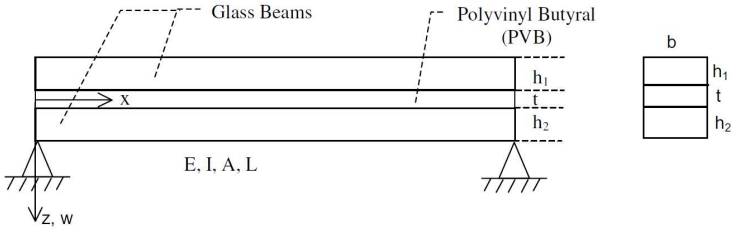

Figure 2: Laminated glass beam [14].

glass	$f(\mathbf{t}_S, \chi_S) = \mathbf{t}_{S_n} - f_{tu} + \chi_S$	$f_{tu} = 40$
PVB	$f(\mathbf{t}_S, \chi_S) = [\mathbf{t}^2_{S_m}]^{0.5} - f_{tu} + \chi_S$	$f_{tu} = 1$

Table 1: Unit materials activation function.

in the top beam. At a certain stage the shear force in the interlayer exceeds its limit value and the irreversible mutual shear displacement takes place, i.e. $[\![\mathbf{u}]\!] \neq 0$ in the PVB as well.

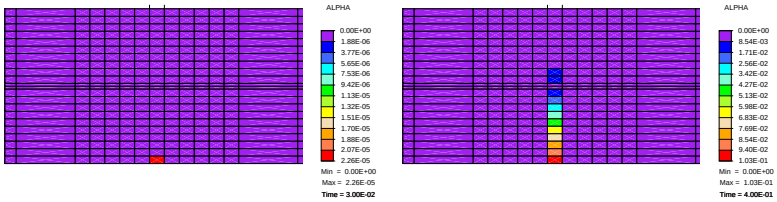

(a) (b)

Figure 3: Laminated beam - SDA prediction of the post post-critic behavior. (a) Initial crack at midspan of the bottom glass beam. (b) Diffusion in the top glass beam.

In order to verify the correct prediction of the initial location of interfaces in the glass layers and in the interlayer, the results are firstly compared with those of a 2D finite element model developed and solved with ADINA code, version 8.4, under the hypothesis of perfect elasticity. A 8-nodes discretization of 800 x (10+2+10) plane stress elements has been used. Indeed, the material has an elastic behavior until interfaces occur, so that, using the activation function in table 1, that at the first stage when $\chi = 0$ is a Rankine-like criterion for glass, cracks rise where the maximum value of the tensile stress is achieved. This first happens at bottom surface of the bottom glass beam.

The results are also commented with reference to the prediction of the mathematical model for the behavior of laminated glass beams of Aşik and Tezcan [14]. It predicts that simply supported laminated glass beams behave close to monolithic glass beams. Their behavior is bounded by two limiting cases which are monolithic and layered behavior. The model, derived by using large deflection theory, shows nonlinear behavior in the case of a fixed supported beam but gives linear

results for a simply supported laminated glass beam. In this latter case it is based on the following differential equation:

$$\frac{d^4 N_1}{dx^4} - \lambda_2 \frac{d^2 N_1}{dx^2} = -\beta q \tag{16}$$

where

$$\lambda_2 = \frac{Gb}{Et}\left(\frac{A_1+A_2}{A_1 A_2} + \frac{h_t^2}{I}\right) \qquad \beta = \frac{Gb}{Et}\frac{h_t}{I} \qquad h_t = \frac{h_1}{2} + \frac{h_2}{2} + t \tag{17}$$

N_1 being the axial force in the top glass layer, E the elastic modulus of glass, G the shear modulus of PVB and I the sum of the moments of inertia of the two glass layers. h_1,h_2 and t are the glass and PVB thickness respectively; b is the unit width. It results $N_1 = -N_2$

The analytic solution gives the following stresses at the surfaces of the plies:

$$\begin{aligned} \sigma_1^{top} &= -\frac{M}{I}\frac{h_1}{2} + \frac{N_1}{A_1} \qquad \sigma_2^{top} = -\frac{M}{I}\frac{h_2}{2} + \frac{N_2}{A_2} \\ \sigma_1^{bottom} &= \frac{M}{I}\frac{h_1}{2} + \frac{N_1}{A_1} \qquad \sigma_2^{bottom} = \frac{M}{I}\frac{h_2}{2} + \frac{N_2}{A_2} \end{aligned} \tag{18}$$

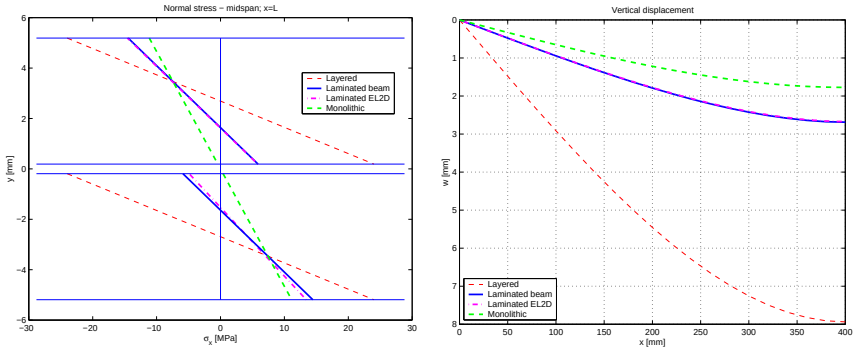

(a) (b)

Figure 4: Aşik and Tezcan model [14] and ADINA solution. (a) Normal stress at midspan. (b) Vertical displacement at midspan.

The behavior for monolithic, laminated and layered beams is illustrated in fig. 4, the transition being influenced by the thickness of the interlayer and its stiffness. The comparison with ADINA simulation is also reported, denoted in the pictures legend as "Laminated EL2D". In the case of coupled response (Laminated) both the analytical model and the ADINA numerical simulation predict that the activation candidate point is the midpoint of the bottom surface, as it is predicted by the SDA simulation of fig. 3.

Model [14] predicts the same curvature for both the glass beams. This result derives from the kinematic hypothesis and is independent on the interlayer stiffness and beam slenderness. Actually, the top beam exhibits a greater curvature than the bottom beam, the difference becoming larger with the decrease of the slenderness and of the interlayer stiffness.

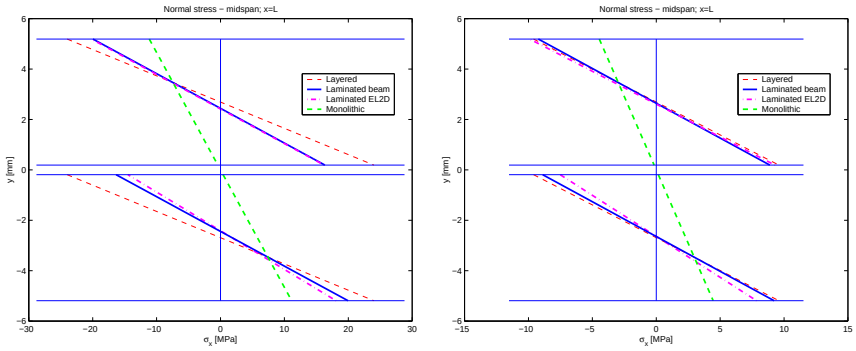

(a)

(b)

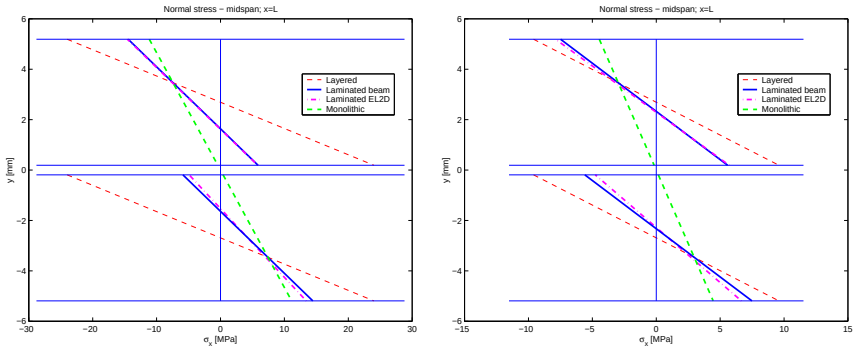

(c)

(d)

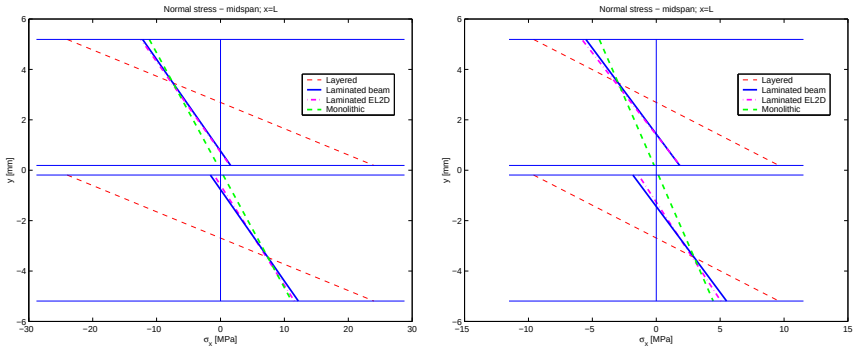

(e)

(f)

Figure 5: Uniaxial stress. Aşik and Tezcan model [14] and ADINA solution. (a) $\rho_1 \simeq 1/80$ - $G = 0.128$ (b) $\rho_2 \simeq 1/32$ - $G = 0.128$ (c) $\rho_1 \simeq 1/80$ - $G = 1.287$ (d) $\rho_2 \simeq 1/32$ - $G = 1.287$ (e) $\rho_1 \simeq 1/80$ - $G = 12.87$ (f) $\rho_2 \simeq 1/32$ - $G = 12.87$

In any case, the behavior is strongly influenced by the stiffness of the interlayer, ranging from layered to monolithic for increasing values of the shear modulus.

In fig. 5 the comparison between the prediction of model [14] and ADINA simulations is reported for two different slenderness ratio $\rho = \frac{(h_1+h_2+t)}{L}$, namely $\rho_1 = \frac{(5+0.38+5)}{800} = 0.0125 \simeq 1/80$ and $\rho_2 = \frac{(5+0.38+5)}{320} = 0.0324 \simeq 1/32$ and three different value of the PVB shear modulus G.

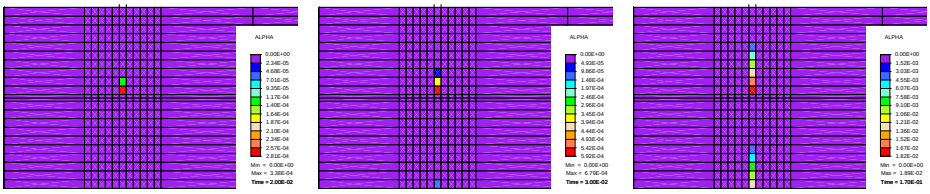

(a) (b) (c)

Figure 6: Laminated deep beam. $\rho = \rho_2 \simeq 1/32$ - SDA prediction of the post post-critic behavior. (a) Initial crack at midspan of the top glass beam. (b) Initial crack at midspan of the bottom glass beam and diffusion in the top glass beam. (c) Diffusion of cracks in glass beams.

In the case of deep beams and low interlayer shear modulus the behavior tends to the layered one and the maximum of the tensile stress is reached at the bottom surface of the top beams. (fig. 5(b)). In this situation the propagation of cracks starts from the upper beam, as it can be observed in fig. 6(a) in which the prediction of the SDA model is reported. The same results is predicted by the ADINA simulation. Successively cracks also arise in the bottom beam (Fig. 6(b)) and follows the same evolution in both the beams (Fig. 6(c)).

5 CONCLUSIONS

A model based on the Strong Discontinuities Approach has been applied to laminated glass beams to simulate the growth and propagation of fracture in a three point bending test. The hypothesis of elastic behavior for both the materials of the composite beam has been formulated, until interface occur, where an elastic-softening behavior is introduced. This is realistic for the glass because it behaves in an elastic-fracturing manner. However, the PVB presents a viscous behavior, that should be enclosed in the model. Nevertheless, the model is able to predict the growth and evolution of cracks inside the layers and gives a good approximation of the stresses in the materials. This initial attempt has to be improved considering more refined constitutive equations.

References

[1] Vallabhan, C. V. G., Das, Y. C., Magdi, M., Asik, M., and Bailey, J. R. "Analysis of lamninated glass units". *Journal of Structural Engineering* **119**(5), 1572–1585 (1993).

[2] Norville, H., King, K., and Swofford, J. "Behaviour and strength of laminated glass". *Journal of Engineering Mechanics* **124**(1), 46–53 (1998).

[3] Benninson, S., Jagota, A., and Smith, C. A. "Fracture of glass-polyvinyl butyral (Butacite) laminates in biaxial flexure". *J. Am. Ceram. Soc.* **82**(7), 1761–1770 (1999).

[4] Foraboschi, P. “Behavior and Failure Strength of Laminated Glass Beams”. *Journal of Engineering Mechanics* **133**(12), 12901301 (2007).

[5] Dharani, L. R., Ji, F., Behr, R. A., Minor, J. E., and Kremer, P. A. “Breakage Prediction of Laminated Glass Using the ””Sacrificial Ply”” Design Concept”. *Journal of Architectural Engineering* **10**(4), 126–135 (2004).

[6] Contrafatto, L. “A variational formulation in damaging plasticity for modelling Strong Discontinuities”. In *Proceedings XIX Congress of the Italian Association for Theoretical and Applied Mechanics* (, Ancona, Italy, 2009). full text on CD ROM.

[7] Simo, J., Oliver, J., and Armero, F. “An analysis of strong discontinuities induced by strain softening in rate independent inelastic solids”. *Computat. Mech.* **12**, 277–296 (1993).

[8] Oliver, J., Cervera, M., and Manzoli, O. “Strong discontinuities and continuum plasticity models: The strong discontinuity approach”. *Int.J. Plasticity* **15**, 319–351 (1999).

[9] Jirásek, M. and Zimmermann, T. “Embedded crack model: Part I: Basic formulation”. *Int. J. Num. Meth. Eng.* **50**, 1269–1290 (2001).

[10] Mosler, J. “A novel algorithmic framework for the numerical implementation of locally embedded strong discontinuities”. *Comp. Meth. App. Mech. Eng.* **194**, 4731–4757 (2005).

[11] Micciché, M. L. *Modeling of cohesive fracture processes through embedded discontinuities*. PhD thesis, University of Catania, Department of Civil and Environmental Engineering, (2006).

[12] Contrafatto, L. and Cuomo, M. “Numerical modelling of growth and propagation of interfaces by means of the embedded discontinuities approach”. In *Proceedings of the 8th. World Congress on Computational Mechanics (WCCM8) and joined 5th European Congress on Computational Methods in Applied Sciences and Engineeering (ECCOMAS 2008)*, Oñate, E. and Owen, D. R. J., editors (, Venice, Italy, 2008). full text on CD ROM.

[13] Taylor, R. *FEAP - A Finite Element Analysis Program*. University of California at Berkeley, Berkeley, California, (2002).

[14] Aşik, M. Z. and Tezcan, S. “A mathematical model for the behavior of laminated glass beams”. *Computers and Structures* **83**, 1742–1753 (2005).